

Relaxation of nonequilibrium soliton structure in incommensurate phase of ferroelectric

V. V. Gladki $\ddot{\text{u}}$, V. A. Kirikov, and E. S. Ivanova

Institute of Crystallography, Russian Academy of Sciences, 117333 Moscow, Russia

(Submitted 13 November 1995)

Zh. Éksp. Teor. Fiz. 110, 298–310 (July 1996)

The evolution of a soliton structure in a dielectric abruptly transformed to a nonequilibrium state and the effect of temperature and defects have been investigated. Evolution proceeds in three stages: an accelerating modification of the structure, when the interaction energy between solitons is higher than the barriers generated by defects; a slow thermally activated relaxation controlled by a logarithmic law, which is typical of many inhomogeneous systems; a much slower relaxation controlled by the diffusion of defects, which generate additional barriers. A phenomenological description of the second stage is given. Relaxation times and heights of barriers in crystals with various contents of defects have been estimated, and these estimates indicate that the relaxation rate is essentially zero after a long time. As an example, dielectric characteristics of Rb_2ZnCl_4 ferroelectric with incommensurate phase are given.

© 1996 American Institute of Physics. [S1063-7761(96)02207-X]

1. INTRODUCTION

The incommensurate phase of a ferroelectric with spontaneous spatially modulated polarization is an example of an inhomogeneous degenerate system which can be studied most efficiently using highly sensitive techniques for measuring electric parameters. At temperatures close to that of the structural transition to the uniform polarized phase, T_c , higher harmonics are detected in the sine-wave modulated polarization of some materials, and the superstructure becomes similar to the ferroelectric domain structure with thin walls (solitons) separating regions with oppositely aligned uniform polarizations (quasi-domains). The period of this soliton lattice and its anomalous dielectric constant with the contribution from soliton oscillations driven by the measuring electric field increase as the temperature approaches T_c .¹

The soliton lattice in a real crystal has a lot of metastable states, transitions between which usually take a long time. For example, if some materials have been kept at a constant temperature for several tens of hours, the state of their soliton lattice is still far from equilibrium. This has been demonstrated by measurements of various physical characteristics, which have an anomalous temperature hysteresis typical of all nonequilibrium systems throughout the region in which the incommensurate phase exists. Owing to the long relaxation time, the soliton lattice is in most cases nonequilibrium during measurements, and the hysteresis, which is usually recorded during one to two hours, is essentially constant in each specific sample. The higher the content of defects in a sample, the larger the hysteresis in it, i.e., the hysteresis width may be used as a measure of the defect content.^{1,2} Thus, measurements of relaxation processes in an incommensurate phase may yield, in principle, not only information about interaction among solitons and between solitons and defects, but also about equilibrium thermodynamic parameters of the soliton lattice.

Many publications have been dedicated to experimental studies of the evolution of soliton lattices. Relaxation was

studied by recording the dielectric constant ϵ or intensity I of x-ray reflections due to the superstructure as functions of time^{3–6} after heating or cooling the sample to a fixed temperature. In such experiments, only the slow stages of relaxation after complete temperature stabilization could be studied, whereas the faster stages were not taken into consideration. The only exceptions were the experiments by Sakata *et al.*,^{7,8} who drove the soliton lattice from the equilibrium state after temperature stabilization using an electric field, and its relaxation was essentially measured from the outset, but their data have not been subjected to quantitative analysis.

Attempts were made^{4,5} to describe the dielectric constant ϵ and structure period l versus time by the function $\epsilon \propto l \propto I \propto \exp(-\sqrt{t/\tau})$ (τ is the relaxation time), and after longer times^{4,6} by the function $\epsilon \propto l \propto I \propto (\ln t)^{-1}$ predicted by the theory^{9,10} describing the kinetics of the nonequilibrium structure in terms of thermally activated growth of solitons. Unfortunately, the accuracy of experimental data was insufficient to verify theoretical predictions.⁶

Earlier^{11,12} we derived from our experimental data a conclusion that the electrically detected relaxation of the soliton lattice in Rb_2ZnCl_4 abruptly switched to a nonequilibrium state proceeds first with acceleration, then more slowly following a logarithmic function of time, which conforms to theoretical predictions^{13,14} based on general ideas about the behavior of solitons in a random medium.

This paper presents an investigation of soliton lattice evolution in samples with various abundances of defects. We have proposed a phenomenological description of the evolution, estimated the relaxation time and energy barriers generated by the defects, and discussed possible reasons for the slow relaxation rate after a long time. The samples were Rb_2ZnCl_4 with the incommensurate phase existing over the temperature range from $T_c = 195.2$ K to $T_i = 303$ K [the modulation wave vector was aligned with the c (or z) axis, and the spontaneous polarization with the b (or y) axis]. The high-temperature phase ($T > T_i$) is described by the spatial symmetry group $Pmcn$, and the low-temperature phase

($T < T_c$) by the $Pn2_1a$ group.¹ The regular soliton structure was directly observed using electron-microscopy techniques.^{15,16}

2. EXPERIMENTAL TECHNIQUES

Uniaxial stress components σ_{yy} and σ_{xx} applied to Rb_2ZnCl_4 shift the temperature T_c of the transition from the incommensurate to polarized phase in opposite directions, namely, σ_{yy} to the low-temperature side, and σ_{xx} to the high-temperature side, i.e., σ_{yy} extends the interval $\Delta T = T - T_c$ between a given temperature of the incommensurate phase and the transition temperature, and σ_{xx} reduces this interval.¹⁷ Given the temperature dependence of the soliton density n ,¹² this means that the compressive stress σ_{yy} leads to a higher soliton density, whereas the stress σ_{xx} reduces the equilibrium density at a fixed temperature $T = \text{const}$.

The possibility of tuning the soliton density n through uniaxial stress was used to switch abruptly an incommensurate soliton structure to another nonequilibrium state near the transition temperature T_c . The measurement procedure was the following. The sample was cooled under a stress $\sigma_{yy} = \text{const}$ or heated under a stress $\sigma_{xx} = \text{const}$ to a given temperature. After the temperature had settled, the stress was removed. As a result, the sample was abruptly switched to a new nonequilibrium state, in the first case with a higher and in the second case with a lower soliton density as compared to its values both in equilibrium and before the stress was removed. The degree of detuning from the equilibrium state was controlled by the applied stress σ_{yy} or σ_{xx} .

Note that uniaxial stress can also be used, first, to switch a sample to a metastable state closer to equilibrium so that the transition should proceed more slowly and, second, to study the effect of stress on the soliton structure relaxation. Thus, the main advantage of uniaxial stress in studies of soliton structure relaxation is the possibility of selecting initial nonequilibrium states over a wide range on both sides of the equilibrium state at any temperature in the range of the incommensurate phase. Besides, unlike the electric field used by Sakata *et al.*,^{7,8} mechanical stress does not change the crystal symmetry, hence it should not change the spatial symmetry of the soliton structure.

The evolution of soliton structure was studied by recording the anomalous dielectric constant ϵ , which is a function of the soliton density n , under an electric field aligned with the y axis.¹ The dielectric constant was measured using a capacitance bridge. The sample faces perpendicular to the y axis were coated with conducting silver paste. The electric field in the sample was constant at $E = 0.5$ V/cm. Before switching the sample to a nonequilibrium state, the bridge was balanced so that the voltage V across its diagonal were zero. During relaxation, the voltage V , which was proportional to the variation of the effective dielectric constant $\delta\epsilon$, was measured. The electric-field frequency was 1 kHz, and $\delta\epsilon$ was plotted by a chart recorder. Given the high speed of the recorder pen (100 cm/s), the time-dependent dielectric response at a rate $\delta\epsilon/\delta t < 600$ s⁻¹ could be recorded. The dielectric constant uncertainty was at most 0.1%, and the temperature was stable to within ~ 0.01 K.

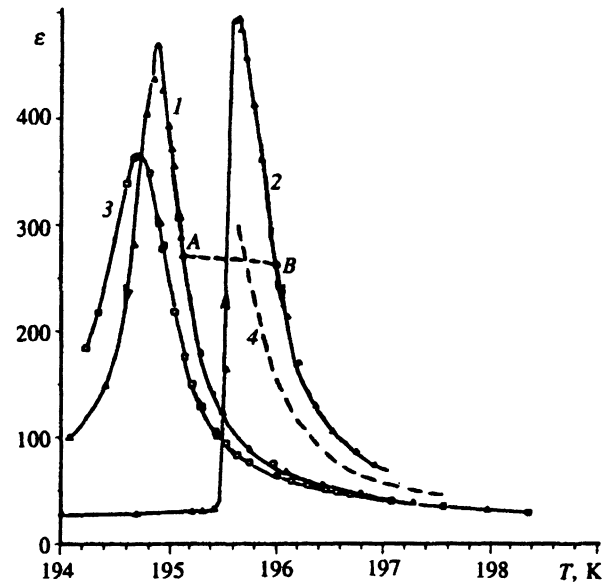


FIG. 1. Dielectric constant ϵ of Rb_2ZnCl_4 vs temperature: 1, 2) strain-free; 3) $\sigma_{yy} = 10$ bar; 4) in thermodynamic equilibrium (ϵ_e). Curves 1 and 3 were recorded during sample cooling, curve 2 when the sample was heated.

If measurements are performed at a fixed temperature for a long time, the crystal “memorizes” this state (structural memory), which can affect subsequent measurements of ϵ at different temperatures.¹ Therefore we performed our measurements under conditions such that the crystal “forgot” its previous state, and the reproducibility of measurements was satisfactory. For example, the crystal was never cooled below T_c , and each relaxation curve in the range of the incommensurate phase was recorded after heating the sample to room temperature and giving it a full day to recover.

At the moment when the stress is lifted, the sample temperature should adiabatically change by $|\delta T| = (\kappa T/c)\sigma$, owing to the piezocaloric effect where κ is the thermal expansion coefficient and c is the specific heat.¹⁸ Given κ and c reported in the literature,¹ we have $|\delta T| = 0.01\text{--}0.02$ K at $\sigma = 5\text{--}15$ bar. When the stress σ_{yy} is removed, the temperature increases ($\delta T > 0$), after the stress σ_{xx} it drops ($\delta T < 0$) in accordance with the opposite signs of the T_c shift due to these stress components. Because of thermal hysteresis, the change in temperature δT leads to a change in ϵ along a flat curve between the points A and B in Fig. 1. The resulting $\delta\epsilon \sim 0.2\text{--}0.4$ is small compared to changes due to relaxation. Therefore, as in the case of an applied electric field,⁷ the dielectric-constant relaxation may be considered an almost isothermal process.

We have studied two samples with various defect abundances, which could be estimated using ϵ at the transition point, ϵ_{\max} , and the temperature hysteresis $(\Delta T)_h$. In the crystal with the lesser content of defects we have $\epsilon_{\max} = 1350$ and $(\Delta T)_h = 0.27$ K, and in that with the higher defect concentration $\epsilon_{\max} = 500$ and $(\Delta T)_h = 0.70$ K. The temperature dependence of ϵ for the second sample is shown in Fig. 1. It also displays the curve of $\epsilon(T)$ recorded under uniaxial stress along the y axis ($\sigma_{yy} = 10$ bar) at decreasing temperature. One can see that uniaxial stress not only shifts

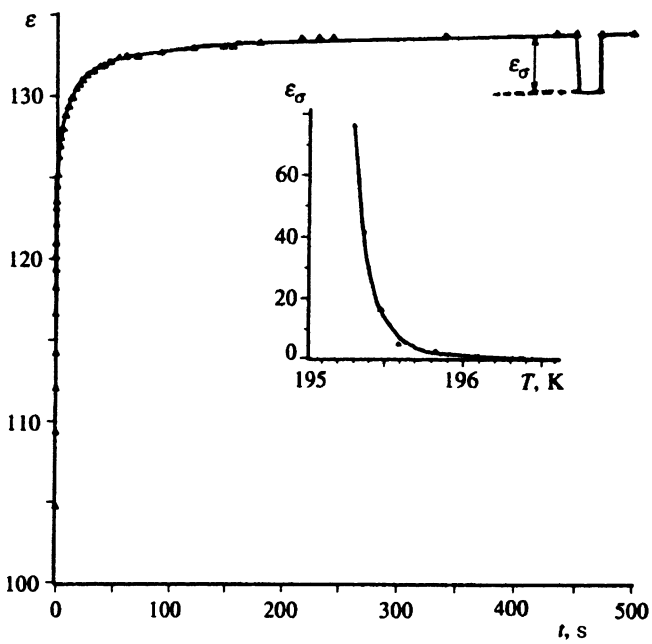


FIG. 2. Dielectric constant ϵ of Rb_2ZnCl_4 versus time at $T = 195.82$ K. The insert shows the temperature dependence of ϵ_σ , which characterizes the drop in the soliton mobility due to mechanical stress σ_{yy} .

the maximum of the $\epsilon(T)$ curve and T_c to lower temperatures, but also reduces ϵ owing to lower soliton mobility in the probe electric field. Figure 2 shows the dielectric-constant relaxation in the first sample recorded under the following conditions: the uniaxial stress was removed at $t=0$ and again applied and removed at $t=450$ s. One can see that the additional stress pulse results in a nearly rectangular pulse with an amplitude $\epsilon_\sigma=3.5$ in $\epsilon(t)$, in which the dielectric constant decreases abruptly owing to a drop in soliton mobility. This short stress pulse has little effect on subsequent relaxation because at this moment the soliton structure is close to its new equilibrium state for a loaded crystal. As a result, the relaxation process is all but interrupted during the stress pulse. The response amplitude ϵ_σ due to lower soliton mobility under stress $\sigma_{yy} \neq 0$ increases as the temperature approaches T_c , from 3.5 at 195.8 K to 75 at 195.3 K (insert in Fig. 2). In this work, we have only studied the dielectric-constant relaxation of a strain-free crystal, and the correction ϵ_σ was always taken into account in determining ϵ at $t=0$.

3. RESULTS AND DISCUSSION

The first change in the nonequilibrium soliton structure is formation of seeds whose soliton density and dielectric constant are different from those of the rest of the sample near electrode surfaces and at other crystal inhomogeneities. Later the seeds grow across the entire sample, whose structure is highly nonuniform throughout the relaxation process until the new equilibrium state is established, and the soliton density is a function of time that is different at each point.¹ The inhomogeneity is obviously related to the various

heights of energy barriers E_g for solitons. For example, E_g is smaller in layers near the electrodes than in the middle of the sample.

A phenomenological description of the dielectric-constant relaxation can be obtained similarly to that of thermally activated changes in magnetization (magnetic viscosity).¹⁹ Suppose that the deviation $\Delta\epsilon$ from the equilibrium value ϵ_e is small, $\Delta\epsilon/\epsilon_e < 1$, and local changes in the electric induction δD , electric field δE , and $\delta\epsilon$ as functions of time are related by

$$\delta D_{\text{loc}} = \bar{E} \delta\epsilon_{\text{loc}} + \bar{\epsilon} \delta E_{\text{loc}}.$$

After integration over unit volume, the second term on the right-hand side is zero, since the local-field variation averaged over the sample is zero, $\bar{\delta E}_{\text{loc}} = 0$, the integral of the first term on the right-hand side over the volume is equal to the integral with respect to the relaxation time τ , and

$$\delta\epsilon_{\text{loc}} = \Delta\epsilon_{\text{max}}(1 - e^{-t/\tau}),$$

where $\Delta\epsilon_{\text{max}} = \epsilon_e - \epsilon_0$, and ϵ_0 is the dielectric constant at $t=0$. As a result, the increment in the effective dielectric constant $\delta\epsilon = \Delta D/E$ is

$$\delta\epsilon = \Delta\epsilon_{\text{max}} \int_{\tau_1}^{\tau_2} p(\tau)(1 - e^{-t/\tau}) d\tau,$$

where $p(\tau)$ is the fraction of the sample volume in which the relaxation time ranges between τ and $\tau+d\tau$, $\tau_1 < \tau < \tau_2$, and $\int_0^\infty p(\tau) d\tau = 1$.

In the simplest case, we assume¹⁹ that the activation energy E_g (hence $\ln \tau$, according to the Arrhenius law $\tau = \tau_0 \exp(E_g/kT)$), is uniformly distributed over the interval between $(E_g)_1$ and $(E_g)_2$; thus we have

$$p(\tau) = \frac{f}{\tau}, \quad \delta\epsilon = \Delta\epsilon_{\text{max}} \left(1 - f \int_{\tau_1}^{\tau_2} \frac{e^{-t/\tau}}{\tau} d\tau \right),$$

or

$$\delta\epsilon = \Delta\epsilon_{\text{max}} - \delta\epsilon = f \Delta\epsilon_{\text{max}} \int_{\tau_1}^{\tau_2} \frac{e^{-t/\tau}}{\tau} d\tau,$$

where $f = 1/\ln(\tau_2/\tau_1)$. The last integral can be expressed in terms of the exponential integral, which can be expanded in series. As a result, we have

$$\delta\epsilon = \begin{cases} \Delta\epsilon_{\text{max}} \left[1 - f \left(\frac{1}{\tau_1} - \frac{1}{\tau_2} \right) t \right], & t \ll \tau_1, \\ \Delta\epsilon_{\text{max}} \tau_2 f \left(\frac{1}{t} \right) e^{-t/\tau_2}, & t \gg \tau_2, \\ f \Delta\epsilon_{\text{max}} [\ln(\tau_2/t) - c], & \tau_1 \ll t \ll \tau_2, \end{cases}$$

where $c = 0.577 \dots$ is Euler's constant.

The latter equation can be transformed to

$$\frac{\Delta\epsilon}{\epsilon_e} - \frac{\Delta\epsilon_0}{\epsilon_e} \approx G \ln \left(\frac{t}{t_0} \right), \quad (1)$$

where $G = -\Delta\epsilon_{\text{max}}/\epsilon_e \ln(\tau_2/\tau_1)$, or

$$\frac{\epsilon_e}{\Delta\epsilon} \approx F + G \ln \left(\frac{t}{t_0} \right), \quad (2)$$

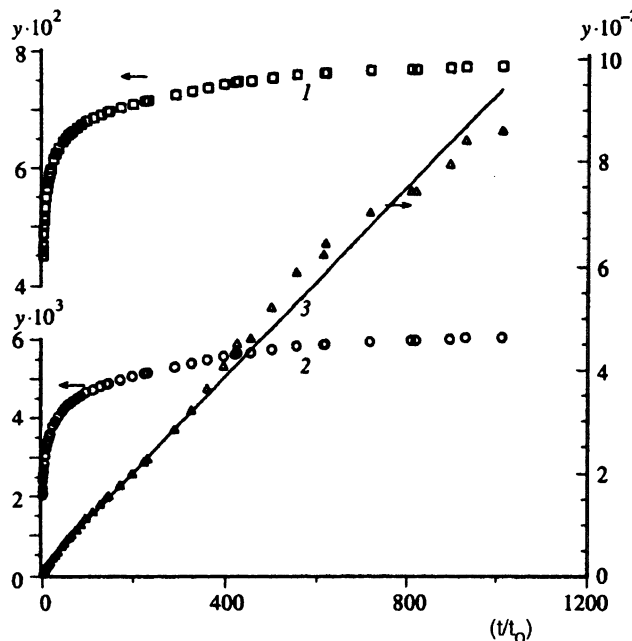


FIG. 3. Experimental curves of ϵ vs time in Rb_2ZnCl_4 plotted to check the three proposed relaxation laws: (1) $y = \ln[(\epsilon_e/\Delta\epsilon)/(\epsilon_e/\Delta\epsilon_{\max})]$; (2) $y = \ln^2[(\epsilon_e/\Delta\epsilon)/(\epsilon_e/\Delta\epsilon_{\max})]$ ^{4,5}; (3) $y = \exp(\epsilon_e/\Delta\epsilon - \epsilon_e/\Delta\epsilon_0)$; $\Delta\epsilon = \epsilon_e - \epsilon(t)$; ϵ_e is the dielectric constant in equilibrium, $\Delta\epsilon_{\max}$ is $\Delta\epsilon$ at $t=0$, $\Delta\epsilon_0$ is $\Delta\epsilon$ at $t=t_0=0.1$ s. Only curve 3 is rectilinear, in accordance with the theory.

where $G = \epsilon_e \ln(\tau_2/\tau_1)/\Delta\epsilon_{\max} \ln^2(\tau_2/t_0)$, t_0 is the time at which the measurements begin, $\Delta\epsilon_0/\epsilon_e$ and $F = \epsilon_e/\Delta\epsilon_0$ are the parameters at $t=t_0$, $\ln(\tau_2/\tau_1) = \Delta E_g/kT$, and $\Delta E_g = (E_g)_2 - (E_g)_1$.

The logarithmic time dependence in Eqs. (1) and (2) holds over a fairly wide time interval if the soliton lattice has only been slightly shifted from its equilibrium state. This is illustrated by Fig. 3, which shows three different functions of ϵ plotted against time. The first curve shows $\epsilon_e/\Delta\epsilon = (\epsilon_e/\Delta\epsilon_{\max})\exp(-t/\tau)$, the second is a plot of $\epsilon_e/\Delta\epsilon = (\epsilon_e/\Delta\epsilon_{\max})\exp(-\sqrt{t}/\tau)$ proposed in Refs. 4 and 5, and the third is the logarithmic function described by Eq. (2). Clearly, only the third curve is rectilinear, whereas the other two are highly nonlinear, i.e., experimental points can be only fitted by the logarithmic function and disagree with the other two proposed equations.

The theory of evolution of a nonequilibrium soliton lattice in crystals with defects, underlying the concept of soliton motion in a random medium, was developed by Kolomeiskii.^{13,14} The specific free energy g of solitons near T_c , where the spacing l between solitons is large, was proposed to be

$$g = -\alpha\Delta T(1/l) + B(1/l)^{\tau+1}.$$

Here, $\Delta T = T - T_c > 0$, $\alpha > 0$, and $B > 0$. The first term on the right-hand side is the energy of attraction between solitons, the second is the repulsion energy, and $\tau \geq 1$ depends on the type of defects present. If the driving force of the relaxation, $F_d = -dg/dl$, is below the threshold determined by dry friction, or the so-called pinning force F_{pin} , and $\Delta\epsilon/\epsilon_e \ll 1$, then one can easily obtain a logarithmic function for $\Delta\epsilon/\epsilon_e$ simi-

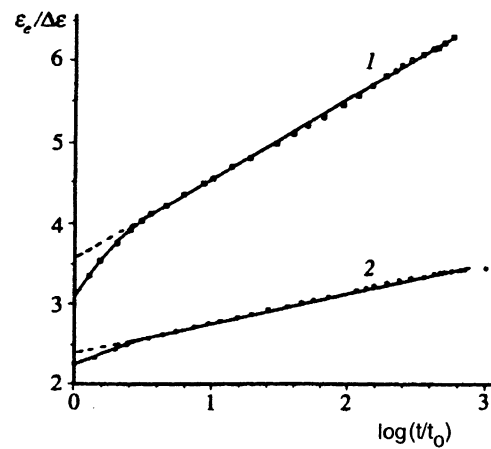


FIG. 4. Logarithmic relaxation of the dielectric constant of Rb_2ZnCl_4 at two temperatures ($T_c = 195.14$ K, $t_0 = 0.1$ s): (1) $T = 195.82$ K; (2) $T = 195.61$ K.

lar to those in Eqs. (1) and (2) with the factor G vanishing at $T \rightarrow T_c$. The theory developed by Kolomeiskii^{13,14} did not take into account electric and elastic long-range forces due to bends in solitons, which can have a considerable effect on thermodynamic^{20,21} and kinetic properties of the crystal. No consistent theory of soliton kinetic properties taking long-range forces into account is presently available.

Below we present measurements of ϵ with initial states characterized by a higher soliton density than in equilibrium. These measurements demonstrate that the temperature, defect concentration, and annealing schedule have a considerable effect on the relaxation process. This also applies to the relaxation of initial states with the soliton density lower than in equilibrium.

Figure 4 shows $\epsilon_e/\Delta\epsilon$ vs $\log(t/t_0)$ for the crystal with the lower defect concentration. When the temperature approaches T_c , the slope of the straight line, given by G in Eq. (2), drops, i.e., the relaxation process becomes slower, as expected.¹⁴

The effect of the defect concentration in a crystal on the relaxation is illustrated by Fig. 5, which shows measurements of ϵ vs time in two samples at equal differences between the measurement temperature and T_c : $\Delta T = T - T_c = 0.52$ K. The slope of the straight line [the factor G in Eq. (2)] is smaller at the higher defect concentration, i.e., the relaxation time is longer.

After long annealing of many crystals at temperature $T_0 > T_c$, additional features emerge in various physical parameters as a function of temperature around T_0 in the incommensurate phase. This memory effect is usually related to the interaction among mobile defects and the resulting structure modulation, hence the defect-density wave, whose wavelength is equal to that of the modulated structure at $T = T_0$. Recent x-ray diffraction studies of thiourea²² indicate that defect-density waves are generated in the incommensurate phase because additional reflections are seen in x-ray diffraction patterns at some temperature T_0 . These reflections can be interpreted in terms of periodic lattice deformation due to defect-density waves.

The redistribution of defects and generation of defect-

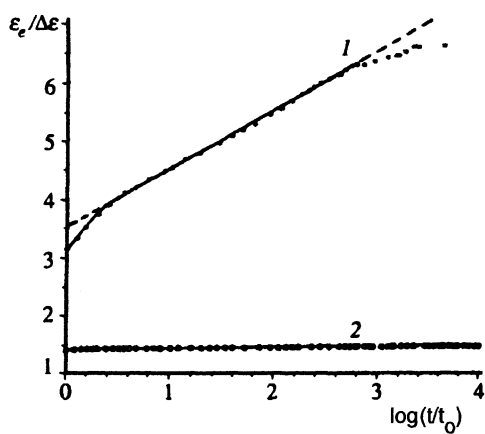


FIG. 5. Logarithmic relaxation of the dielectric constants of two Rb_2ZnCl_4 samples with different defect concentrations: (1) sample with the lower defect concentration, $T_c = 195.14 \text{ K}$; (2) sample with the higher defect concentration, $T_c = 194.84 \text{ K}$; $\Delta T = T - T_c = 0.52 \text{ K}$ for both samples.

density waves should modify the heights of the energy barriers E_g and, hence, the relaxation time τ . Figure 6 shows ε vs time and $\varepsilon_e/\Delta\varepsilon$ vs $\log(t/t_0)$ for samples with various defect concentrations annealed at temperatures T_0 equally separated from the transition point T_c : $\Delta T = T_0 - T_c = 0.52$

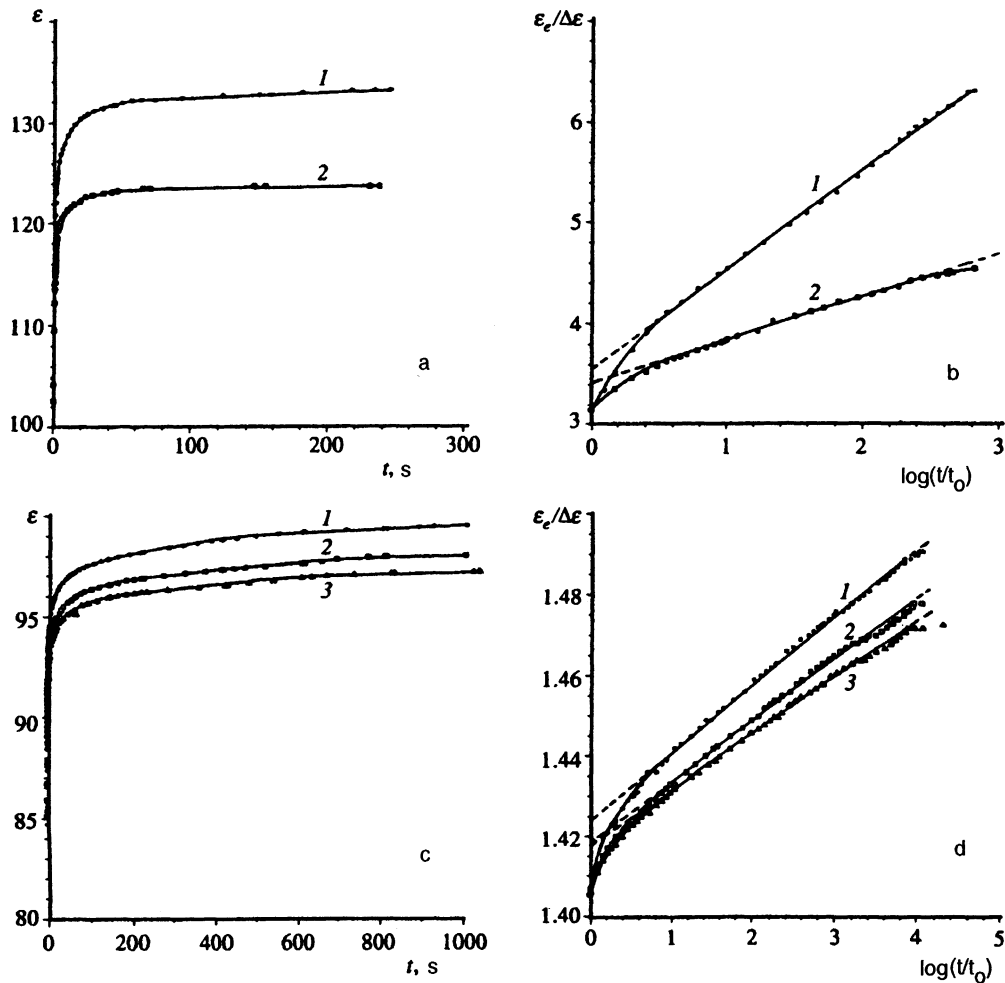


FIG. 6. Dielectric constant ε vs time t and $\varepsilon_e/\Delta\varepsilon$ vs $\log(t/t_0)$ after annealing at the temperature T_0 in Rb_2ZnCl_4 samples with various defect concentrations: a and b) lower defect concentration; c and d) higher defect concentration; (1) annealing time $t_{\text{an}} = 10 \text{ min}$; (2) $t_{\text{an}} = 1 \text{ h}$; (3) $t_{\text{an}} = 2 \text{ h}$.

TABLE I. Estimates of the parameter G , $(E_g)_2$, ΔE_g , τ_1 , τ_2 , for samples of Rb_2ZnCl_4 with lower (1) and higher (2) concentration of defects.

Sample	$G \cdot 10^2$	$(E_g)_2$, eV	ΔE_g , eV	τ_1 , s	τ_2 , s
1 $T = 195.82 \text{ K}$	45 ± 2	0.7 ± 0.1	0.6 ± 0.1	$10^{-6} - 10^{-11}$	$10^5 - 10^6$
1 $T = 195.61 \text{ K}$	15 ± 1	0.8 ± 0.1	0.59 ± 0.09	$10^{-4} - 10^{-9}$	$10^8 - 10^9$
1 $T = 195.82 \text{ K}$ $t_{\text{an}} = 2 \text{ h}$	22 ± 1	0.9 ± 0.1	1.00 ± 0.15	$\ll 10^{-10}$	$10^9 - 10^{11}$
2 $T = 195.65 \text{ K}$	0.9 ± 0.1	3.6 ± 0.3	3.9 ± 0.6	$\ll 10^{-10}$	$\gg 10^{11}$
2 $T = 195.65 \text{ K}$ $t_{\text{an}} = 3 \text{ h}$	0.8 ± 0.1	4.0 ± 0.3	4.2 ± 0.7	$\ll 10^{-10}$	$\gg 10^{11}$

by varying $\varepsilon_e/\Delta\varepsilon_e$ with respect to ε_e . For example, the correction to $\varepsilon_e/\Delta\varepsilon$ in Eq. (2) that is quadratic in $\ln(t/t_0)$ equals $G^2(\delta\varepsilon_e/\varepsilon_e)\ln^2(t/t_0)$, i.e., the deviation from the logarithmic curve at $\delta\varepsilon_e/\varepsilon_e \neq 0$ increases with time:

$$\frac{\delta F}{F} = (1-F) \frac{\delta\varepsilon_e}{\varepsilon_e}, \quad \frac{\delta G}{G} \approx (-2F+1) \frac{\delta\varepsilon_e}{\varepsilon_e},$$

$$\frac{\delta\varepsilon_e}{\varepsilon_e} = \left[(F-1) - G \ln\left(\frac{t}{t_0}\right) - \frac{G^2}{b} \ln^2\left(\frac{t}{t_0}\right) \right]^{-1},$$

where b is the deviation of $\varepsilon_e/\Delta\varepsilon$ from the straight line at time t . Estimates derived from these formulas, however, indicate that the observed deviations of experimental points from the straight line are not caused by the uncertainty $\delta\varepsilon_e/\varepsilon_e$ in choosing ε_e , and $\delta\varepsilon_e/\varepsilon_e$ is small. For example, in the case of curve 1 in Fig. 5 we have $G \approx 1$ and $F = 3.5$; at $\log(t/t_0) = 3$ the deviation $b \leq 0.1$, $\delta\varepsilon_e/\varepsilon_e \leq 0.002$, $\delta F/F \leq 0.005$, and $\delta G/G \leq 0.01$. In order to obtain the deviation $b \approx 0.6$, which takes place in Fig. 5 at $\log(t/t_0) \approx 3.5$, an enormous time would be required: $\log(t/t_0) \approx 18$ ($t_0 = 0.1 \text{ s}$).

The relaxation times of the soliton lattice and heights of barriers due to defects can be estimated using experimental data and Eqs. (1) and (2). Table I lists these estimates for the two samples with the lower (1) and higher (2) concentrations

of defects. Above all, note that Eqs. (1) and (2) will be valid at any time limited by the condition $\tau_1 \ll t \ll \tau_2$. The maximum barrier heights $(E_g)_2$ are derived from the equation $\tau_2 = \tau_0 \exp[(E_g)_2/kT]$ at $\tau_0 = 10^{-7} - 10^{-11} \text{ s}$. The width ΔE_g of the interval over which the barrier height is distributed equals $(E_g)_2$, within the experimental uncertainty i.e., the lower bound for $(E_g)_1$ is essentially zero. Table I indicates that the barrier height and relaxation time τ_2 increase when the temperature approaches T_c , when the defect concentration increases, and after annealing. In the second sample with the higher defect concentration, the barrier heights are about 4 eV, and relaxation time τ_2 is so enormous that the relaxation process essentially stops long before thermodynamic equilibrium is achieved.

Thus, the experimental data and estimates of the relaxation time and activation energy indicate once again that defects and their redistribution due to diffusion during annealing determine the barrier heights for soliton structure and have a dominant effect on its long-time relaxation.

Measurements of $\varepsilon_e/\Delta\varepsilon$ deviate from the logarithmic curves not only at very large, but also at small times (Figs. 4–6). These deviations are seen most clearly when ε is measured at different initial states of the soliton structure. Figure 7 shows measurements of the sample with the higher defect

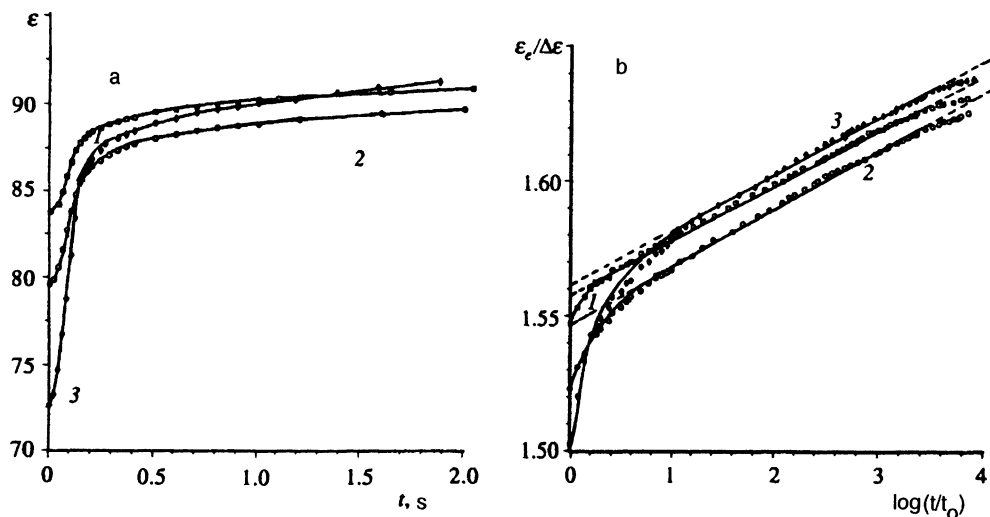


FIG. 7. (a) Dielectric constant ε vs time t and (b) $\varepsilon_e/\Delta\varepsilon$ vs $\log(t/t_0)$ for Rb_2ZnCl_4 in various initial non-equilibrium states. $T_c = 194.84 \text{ K}$, $\Delta T = T - T_c = 0.52 \text{ K}$, $\varepsilon_e = 266.3$. The compressive stress σ_{yy} generating nonequilibrium states is (1) 7.5 bar, (2) 10 bar, and (3) 20 bar.

concentration. One can see that during rapid evolution the rate of ε increases, then drops and follows the logarithmic curve. The further the initial state from equilibrium, the larger the rate of ε and the closer to equilibrium the system at the onset of slow logarithmic evolution; therefore the curves of ε vs t and of $\varepsilon_e/\Delta\varepsilon$ vs $\ln(t/t_0)$ intersect. It is obvious that the rate of both ε and average soliton spacing l increase until the thermodynamic driving force $F_d = -dg/dl$ (where g is the free energy), which decreases as the system approaches its equilibrium state, is larger than the dry friction, or pinning force F_{pin} , due to defects. The rate of change is maximum at $F_d = F_{\text{pin}}$. At $F_d < F_{\text{pin}}$, soliton structure evolution becomes slower and is controlled by thermally activated processes. In the second sample with the lower defect concentration, the fast process proceeds similarly. If we assume that F_d is approximately proportional to $\Delta\varepsilon/\varepsilon_e$, it follows from our data that at $F_d = F_{\text{pin}}$, where the derivative $d\varepsilon/dt$ is maximum, the ratio of friction forces averaged over volume in the first and second samples equals 2.

Note that the first, faster stage of the evolution has much in common with the repolarization of ferroelectrics and remagnetization of ferromagnetics. It is also possible that these processes are controlled by the same mechanism, namely the displacement of inhomogeneous regions (domain walls²³ or solitons) with acceleration and subsequent deceleration, similar to the motion of a pendulum with large dry friction.

4. CONCLUSION

Using our experimental data, we have outlined the evolution of the nonequilibrium soliton structure in the ferroelectric Rb_2ZnCl_4 . Evolution proceeds in three stages, controlled by various mechanisms. In the first, fast stage, the free energy of the soliton system exceeds the height of barriers due to defects, and motion is accelerated. In the second stage, the process is retarded by defects and proceeds slowly, with a logarithmic time dependence of system parameters. The third, slowest stage of the process is accompanied by the restructuring of the defect pattern due to diffusion, leading to higher energy barriers for the soliton structure, which results essentially in the termination of the relaxation process. More information can be derived in the first two stages of evolution, namely the ranges of relaxation times and barrier heights, and the dielectric constant in equilibrium states, which are essentially never achieved in a soliton structure,

measured in samples with various defect concentrations. The equilibrium parameters may be useful in studies of critical behavior of the soliton lattice. The duration of the first two stages is usually several minutes, and they can only be studied if the soliton structure can be abruptly switched to a nonequilibrium state in each sample. The soliton structure in Rb_2ZnCl_4 studied in our work is a typical representative of its class, and information about its kinetic properties can be applied to other nonuniform systems.

We are indebted to A. P. Levanyuk and S. A. Minyukov for helpful discussions. The work was supported by INTAS (Grant No. 93-03230) and Russian Fund for Fundamental Research (Project No. 93-02-14163).

- ¹H. Z. Cummins, Phys. Rep. **185** (5, 6), 211–409 (1990).
- ²K. Hamano, H. Sakata, K. Yoneda *et al.*, Phase Transitions **11**, 279 (1988).
- ³G. Zhang, S. L. Qiu, M. Dutta, and H. Z. Cummins, Sol. St. Commun. **55**, 275 (1985).
- ⁴H. Mashiyama and H. Kasatani, J. Phys. Soc. Jap. **56**, 3347 (1987).
- ⁵S. A. Gridnev, V. V. Gorbatenko, and B. N. Prasolov, Kristallografiya, **39**, 21 (1994).
- ⁶K. Ema, K. Hamano, and H. Mashiyama, J. Phys. Soc. Jap. **57**, 2174 (1988).
- ⁷H. Sakata, K. Hamano, and K. Ema, J. Phys. Soc. Jap. **57**, 4242 (1988).
- ⁸K. Hamano, H. Sakata, and K. Ema, Ferroelectrics **137**, 235 (1992).
- ⁹K. Kawasaki, J. Phys. C **16**, 6911 (1983).
- ¹⁰K. Kawasaki, Physica B **124**, 156 (1984).
- ¹¹V. V. Gladkiĭ, V. A. Kirikov, and E. S. Ivanova, Pis'ma Zh. Éskp. Teor. Fiz. **58**, 625 (1993).
- ¹²V. V. Gladkiĭ, V. A. Kirikov, and E. S. Ivanova, Pis'ma Zh. Éskp. Teor. Fiz. **60**, 109 (1994).
- ¹³E. B. Kolomeškiĭ, Zh. Éskp. Teor. Fiz. **99**, 546 (1991).
- ¹⁴E. B. Kolomeškiĭ, Ferroelectrics **105**, 131 (1990).
- ¹⁵H. Bestgen, Sol. St. Commun. **58**, 197 (1986).
- ¹⁶K. Tsuda, N. Yamamoto, and K. Yadi, J. Phys. Soc. Jap. **57**, 2057 (1988).
- ¹⁷V. V. Gladkiĭ, V. A. Kirikov, I. S. Zheludev, and I. V. Gavrilova, Fiz. Tverd. Tela **29**, 1690 (1987).
- ¹⁸J. Nye, *Physical Properties of Crystals. Their Representation by Tensors and Matrices*, Oxford University Press, Oxford (1964).
- ¹⁹S. Krupička, *Physik der Ferrite und der Verwandten Magnetischen Oxide* [in German], Academia, Praha (1973).
- ²⁰E. B. Kolomeškiĭ, A. P. Levanyuk, and S. A. Minyukov, Fiz. Tverd. Tela **3**, 545 (1988).
- ²¹E. B. Kolomeškiĭ, A. P. Levanyuk, and A. S. Sigov, Ferroelectrics **104**, 195 (1990).
- ²²B. Sh. Bagautdinov and I. M. Shmyt'ko, Pis'ma Zh. Éskp. Teor. Fiz. **59**, 171 (1990).
- ²³M. Lines and A. Glass, *Principles and Applications of Ferroelectrics and Related Materials*, Oxford University Press, Oxford (1977).

Translation was provided by the Russian Editorial office.